Articles in PresS. J Neurophysiol (October 9, 2013). doi:10.1152/jn.00593.2013

TITLE PAGE

Title

Central complex neurons exhibit behaviorally gated responses to visual motion in *Drosophila*

Authors

Peter T. Weir[1], Bettina Schnell[1], Michael H. Dickinson[1]

1. Department of Biology, University of Washington, Seattle, WA

Abbreviated title

Behaviorally gated neuronal responses to visual motion

Corresponding Author

Michael H. Dickinson

flyman@uw.edu

UW Biology

Box 351800

24 Kincaid Hall

Seattle, WA 98195-1800

office: (206) 221-1928

ABSTRACT

Sensory systems provide abundant information about the environment surrounding an animal, but only a small fraction of that information is relevant for any given task. One example of this requirement for context-dependent filtering of a sensory stream is the role that optic flow plays in guiding locomotion. Flying animals, which do not have access to a direct measure of ground speed, rely on optic flow to regulate their forward velocity. This observation suggests that progressive optic flow, the pattern of front-to-back motion on the retina created by forward motion, should be especially salient to an animal while it is in flight, but less important while it is standing still. We recorded the activity of cells in the central complex of *Drosophila melanogaster* during quiescence and tethered flight using both calcium imaging and whole-cell patch-clamp techniques. We observed a genetically identified set of neurons in the fan-shaped body that are unresponsive to visual motion while the animal is quiescent. During flight their baseline activity increases and they respond to front-to-back motion with changes relative to this baseline. The results provide an example of how nervous systems selectively respond to complex sensory stimuli depending on the current behavioral state of the animal.

KEYWORDS

Context, task-dependent, flight, fan-shaped body, optic flow

INTRODUCTION

The pattern of light impinging on an animal's retina contains critical information about the world as well as unimportant distractions. Animals have evolved visual systems that are capable of detecting important features, but the relevance of a given stimulus may depend on an animal's current behavioral state. For example, the appearance of a rapidly expanding object triggers wing elevation, leg positioning, and take-off when a fly is standing still (Hammond and O'Shea 2007; Card and Dickinson 2008), but an identical stimulus elicits an evasive turn when the animal is flying (Bender and Dickinson 2006). Such task-

dependent visual processing is likely ubiquitous among eyed organisms. One type of stimulus that is especially relevant to locomotion is the global pattern of movement of elements in the visual surround, termed optic flow, which results from an animal's motion through the environment (Gibson 1958). When the animal rotates it experiences purely rotational optic flow, in which features on the retina move at an angular velocity independent of their distance from the animal. In translational optic flow the pattern appears to expand from a point in the direction of the animal's movement. Hence, an organism can use optic flow to monitor its own motion through the world, a process that is critical for many behaviors including speed control and visual odometry (Srinivasan et al. 1997; Baird et al. 2005; Fry et al. 2009). Translational optic flow is further categorized as either progressive, resulting from forward movement, or regressive, resulting from backward movement (Koenderink 1986).

The neural circuits underlying motion vision in flies have been studied extensively (e.g. Joesch et al. 2010; Clark et al. 2011; Paulk et al. 2013). It is unknown, however, where output from the optic lobes is combined with other information to trigger or modulate behavior. One candidate for such a region is the central complex, a set of structures including the protocerebral bridge, fan-shaped body, ellipsoid body, and noduli (Loesel et al. 2002; Strausfeld and Hirth 2013). Electrophysiological evidence from other species suggests that the central complex plays a role in spatial navigation and leg coordination, among other behaviors (Vitzthum et al. 2002; Bender et al. 2010). It receives indirect visual input and contains output neurons whose terminals overlap with dendrites of descending interneurons (Homberg 2004). In this study, we examined the responses of the ExFl1 (alternately F1) neurons, a class of approximately seven bilateral pairs with cell bodies in the anterior cortex, putative presynaptic terminals (outputs) in the ventral-most layer of the fan-shaped body, putative postsynaptic processes (inputs) in the ventral body, and processes of unknown polarity in the inferior medial protocerebrum (Li et al. 2009; Young and Armstrong 2010). We recorded the activity of these cells during quiescence and flight using both two-photon excitation of genetically encoded calcium indicators and whole-cell patch-clamp

electrophysiology. Using both methods, we observed responses to changes in translational optic flow during flight, but no responses during quiescence.

MATERIALS AND METHODS

Animals

All flies included in our experiments were 1- to 6-day-old females raised on a standard cornmeal medium and a 14hr/10hr light/dark cycle at 25° C. We anesthetized each fly by cooling it to 4° C and then removed the pro- and meso-thoracic legs at the coxa/trochanter joint and the tibia and tarsi of the metathoracic legs to prevent tarsal contact with the fly mount. (Such contact leads to diminished flight initiation and duration.). We then glued the head to a custom holder with ultraviolet-cured glue and fixed the proboscis in place with additional glue (Fig. 1*A,B*). Immediately prior to each experiment, we dissected a small hole in the cuticle in extracellular saline with a hypodermic needle. In imaging experiments, the fly's head was tilted forward, such that the posterior side of the head was roughly 15° above horizontal and the eyes were entirely exposed to the area below the holder. In order to access the cell somata in electrophysiology experiments, however, it was necessary to tilt the fly's head back and dissect through the rostral side of the head capsule, just dorsal to the antennae. In this configuration, approximately a dorsal third of the compound eyes were occluded by the holder.

Fly strains

We used the following parental fly strains in our experiments (generously provided by the source in parentheses): NP6510, denotes genotypes: y[*] w[*]; +; P{GawB}NP6510 or +; +; P{GawB}NP6510 (Dr. Angelique Paulk, University of Queensland, St. Lucia, Queensland), GCaMP3 denotes genotype: +; pJFRC-MUH{UAS-GCaMP3.0}attP40; + (Dr. Allan Wong, California Institute of Technology, Pasadena, CA), eGFP denotes genotype +; P{w[+mC]=UAS-2xEGFP}AH2; + (Dr. Allan Wong, California Institute of Technology, Pasadena, CA), GCaMP5 denotes genotype +; PJFRC7-20xUAS-

GCaMP5.003 in attP40; + (Dr. Loren Looger, Janelia Farm Research Campus, Ashburn, VA). Each fly used in our experiments was heterozygous with at least one wildtype copy of each chromosome.

Two-photon imaging

Methods for two-photon imaging in behaving flies have been described previously (Seelig et al. 2010; Suver et al. 2012).We imaged *in vivo* fluorescence of GCaMP3 and GCaMP5 (Tian et al. 2009; Akerboom et al. 2012) with a Prairie Ultima IV two-photon microscope equipped with a Nikon 40x NIR Ap objective water-immersion lens (0.8 NA). In each preparation, we located the fan-shaped body terminals of the ExFl1 cells, which are easily identified due to the sparseness of expression in the NP6510 driver line (Fig. 1*C,D*), and are known to be a localization site of presynaptic proteins in the cells (Li et al. 2009). We used an excitation wavelength of 930 nm and limited imaging to a 79.4 x 52.9 μm region with less than 37 mW laser power. (This value was measured at the rear aperture of the objective lens, but without the objective or saline in place, so it is necessarily an overestimate of actual laser power delivered during experiments.) The excitation laser dwelled on each 0.66 x.66 μm pixel for 4 μs and we scanned the entire area at 16.1 frames per s. We collected fluorescence using a multi-alkali photomultiplier tube (Hamamatsu) after bandpass filtering it with an HQ 525/50m-2p emission filter (Chroma Technology). We acquired data in blocks of 1700 frames (106 s), between which the excitation laser was off. After 13 blocks we recorded a depth stack to verify the location of our imaging region. In total we recorded from 22 flies expressing GCaMP3, 28 flies expressing GCaMP5, and 8 flies expressing eGFP.

Imaging data analysis

We performed all analyses in Python. We first computed the mean of all (22100) frames from each animal. We classified the region of interest (ROI) as the brightest 10% of pixels in this mean image, an area large enough to encompass most of the GCaMP-expressing processes in the imaging window, and the dimmest 10% of pixels were classified as background (Fig. 1*D*). For each frame, we computed fluorescence (F_t) by subtracting the sum of the background pixels from the sum of the ROI pixels (Fig.

1*E*). For each fly, we computed the mean F_t before stimulus onset for each trial in which the fly did not fly (F_0). Our metric for response, plotted in Figures 2-5, is $(F_t - F_0)/F_0$, which we call $\Delta F/F$ for brevity.

Electrophysiology and immunohistochemistry

The method for whole-cell patch-clamp recordings in behaving flies has been reported previously (Maimon et al. 2010). Briefly, we ruptured the lamella using a micropipette containing 0.5 mg ml^{-1} collagenase and localized mechanical abrasion. Both collagenase de-sheathing and patch-clamp recordings were performed at 22°C bath temperature. Recording electrodes had a resistance of 8-10 MOhm and were filled with intracellular solution containing 13 mM Biocytin hydrazide (Invitrogen #B1603) and 20 μM A568-hydrazide-Na (Invitrogen, #A-10437) to visualize cells after recording. Once in whole-cell configuration, we recorded membrane potential using an A-M Systems 2400 amplifier and Axoscope software sampling at 10 kHz. The access resistance to the cells was less than 50 MOhm at the beginning of every recording. In one case, we injected a small hyperpolarizing current (-0.018 nA) into the cell to stabilize its membrane potential, which led to a resting spike frequency and membrane potential comparable to those observed in the other recordings. After recording, we dissected the brain and fixed it for 1h in 4% paraformaldehyde. Subsequently, we first stained each preparation with antibodies against GFP (1:1000, rabbit, Invitrogen) and NC82 (1:10, mouse, Developmental Studies Hybridoma Bank) and then applied goat anti-mouse Alexa Fluor 633 (1:250, Invitrogen), goat anti-rabbit Alexa Fluor 488 (1:250, Invitrogen), and streptavidin-Alexa Fluor 568 (1:1000, Invitrogen) overnight at 4°C. To confirm that the recorded cells were GFP-positive we scanned brains using a confocal microscope (Leica SP5 II) with a 40x oil-immersion objective at a step size of 0.5 μm (Fig. 1*C*). We used ImageJ to adjust the brightness and contrast of the images. We recorded from 22 neurons (each in a different animal) in total, 14 of which were GFP-positive. Of those 14 recordings, 7 flies flew a minimum of four repetitions of each trial type and were included in our analysis.

Electrophysiology data analysis

We corrected for the junction potential by subtracting 13 mV from the values in the raw recordings. To identify action potentials we filtered raw membrane potential with a third order Butterworth bandpass filter with cutoff frequencies of 5 Hz and 1000 Hz. We then down-sampled the data to a sample rate of 1000 Hz. For most recordings, a simple threshold applied to the filtered potential sufficed to determine spike times, but for several recordings we added a requirement on rise time to distinguish changes in potential close to the threshold. To compute an estimate of instantaneous spike rate (Figs. 2 and 4) we averaged across trials using a Gaussian window with a standard deviation of 75 ms to diminish the fluctuations due to the high variability in the spike data (other researchers have used 200 ms standard deviation Gaussian windows, eg. Rosner and Homberg 2013).

Stimuli

During all imaging experiments, we continuously displayed visual patterns in pseudorandom order using a 32-tall x 96-wide array of blue LEDs (470 nm peak wavelength). The array was arranged in a partial cylinder centered on the fly, aligned perpendicularly to the horizontal axis of the fly's head. It covered from 32° below to 32° above the horizontal and 108° to either side of the fly's midline (Fig. 1*I*). Three layers of blue filter (Rosco #59 Indigo) above the LED array prevented light from leaking through the microscope's bandpass filter cube and into the photomultiplier. To eliminate the potentially confounding effects of any remaining light leaks, we used entirely isoluminant patterns in the first two experiments. Thus, the patterns were programmed such that when dark objects appeared, the background luminance increased uniformly to maintain constant LED light output. In the last experiment bright spots moved on a dark background and the average stimulus luminance was less than 14% of that in the earlier experiments, contributing negligible background light. We elicited flight by delivering a 200 ms puff of air at the fly from a vacuum pump (Cole-Parmer) controlled by an electronic solenoid valve.

In electrophysiology experiments we used a similar stimulus display, except that the LEDs emitted green light (570 nm peak wavelength), and they covered an area from approximately 0° to 64° below and from 117° to the right to 81° to the left of the fly.

Behavioral monitoring

Infrared LEDs (850 nm peak wavelength) illuminated the fly from the posterior direction. An infrared-sensitive camera recorded images of the fly from below at 40-50 frames per s, and custom software calculated the amplitude of the left and right wing stroke envelopes in each frame (Maimon et al. 2010). Figure 1*B* shows an example frame. For each frame, we computed the difference and the sum of the two wing stroke amplitudes (denoted L-R and L+R, respectively, Fig. 1*F*,*G*). This behavioral data allowed us to unambiguously identify when each animal was flying. For some trial-by-trial analyses, we subtracted the mean during the 0.5 s before stimulus onset from these values to compute the stimulus-induced changes, which we term Δ(L-R) and Δ(L+R), respectively.

Nomenclature

Liu et al. (2006) refer to the ExFl1 and ExFl2 neurons as the F1 and F5 neurons, respectively, because they innervate layers 1 and 5 of the fan-shaped body. The six fan-shaped body layers are labelled from ventral (1) to dorsal (6). Here we have adopted the naming convention of Young and Armstrong (2010), because F1 (F-one) is easily confused with Fl (F-lowercase L), which was used by Hanesch et al. (1989) to distinguish fan-shaped body (F) neurons whose axon is lateral to the ellipsoid body from F neurons whose axons traverse the median canal of the ellipsoid body. Further complicating matters, in some insects the fan-shaped body is called the central body upper division and the ellipsoid body is called the central body lower division. We use the *Drosophila* nomenclature throughout, with apologies to researchers accustomed to the other convention. Finally, all anatomical coordinates refer to the body and head axes (to convert to the neuraxis convention, substitute the anterior/posterior axis for our dorsal/ventral axis).

RESULTS

Within the central complex of *Drosophila* the driver line NP6510 selectively expresses Gal4 in ExFl1 neurons (Fig. 1*C*), a class of tangential neurons, whose output terminals cover layer 1 of the fan-shaped body (Young and Armstrong 2010). In a tethered preparation (Fig. 1*A*) we recorded ExFl1 neuronal activity in the fan-shaped body using GCaMP3 and GCaMP5 during flight and quiescence in the presence of visual stimuli. In addition we performed whole-cell patch-clamp recordings from the somata of single ExFl1 neurons.

Baseline activity of ExFl1 neurons increases during flight

It has previously been reported that neurons in the optic lobes display increased activity when the animal is flying or walking compared to when it is quiescent (Chiappe et al. 2010; Maimon et al. 2010; Jung et al. 2011). This increase is composed of two parts, a tonic shift in the baseline membrane potential of the cells, and an increased gain in response to motion of the visual stimulus. Similarly, we examined the effect of flight on ExFl1 neurons both independent of visual stimulation and in response to visual motion. The baseline activity of ExFl1 neurons during quiescence was stable and the cells showed no response to the visual stimuli we presented. This observation held whether surveying the activity with GCaMP3, GCaMP5, or intracellular recordings. When we elicited flight (Fig. 2*B*) with a gentle air puff, however, these cells increased their activity by all three measures (Fig. 2*A*). The activity remained above baseline for the duration of flight, then decreased when the fly stopped flying. The changes in spike rate, though small in magnitude, correspond well to the changes reported by GCamp3 and GCamp5. As a control for movement artifacts, we expressed GFP using the same driver line. These flies initiated flight normally, but exhibited no concomitant change in fluorescence.

Neuronal activity is modulated by translational optic flow in flying flies

In addition to studying flight-induced changes in baseline activity of the ExFl1 neurons, we examined the effect of flight on the visual responses of these cells. Flies experience translational and rotational optic flow due to their own motion during flight and use these stimuli for course control. Salient objects, such

as vertical bars, also elicit robust positional and directional responses in flies (Reichardt and Poggio 1976; Götz 1987; Bahl et al. 2013). As the central complex has been implicated in visual navigation, we reasoned that these features might be processed by cells in this brain region. We therefore simulated rotational and translational motion using simple combinations of vertical black bars.

During flight, the ExFl1 cells responded robustly to horizontally moving patterns. Using GCaMP3, we recorded changes in presynaptic calcium in response to four trial types. Each trial began with the appearance of one or more dark vertical stripes, 18° wide, which then oscillated horizontally for 4 s at 0.5 Hz with 45° peak-to-peak amplitude. The velocity of the stripes was modulated sinusoidally starting at the phase of maximum speed. In the first trial type, one stripe oscillated in one half of the visual field, centered at 45° in the right hemi-field of the fly (Fig. 3, first column). In the next trial type, two such stripes, one in the left and the other in the right visual field of the fly, oscillated in phase, simulating rotational motion (Fig. 3, second column). The third trial type was identical to the second, but an additional stripe was located midway between the first two stripes (Fig. 3, center column). In the fourth trial type, two stripes oscillated in anti-phase simulating translational motion (Fig. 3, fourth column). Although relatively simple, these stimuli can be divided into three types of global optic flow that should provide functionally relevant interpretations of self-motion. When two or three stripes move in phase, the resulting optic flow should indicate rotation; when two stripes move in opposite phases, the optic flow should indicate translation. In the trials with just one stripe, the stimulus is ambiguous with respect to rotation and translation.

We recorded from 12 flies that flew a minimum of nine repetitions of each trial type. (See Fig. 1*E*-*G* for individual trials of a single fly.) For a trial to be included in the analysis, we required continuous flight from 0.5 s before the pattern appeared until 3 s after it disappeared. Usually flies flew continuously for many successive trials. In response to rotational optic flow, the flies exhibited changes in the difference between their left and right wing stroke amplitudes (Δ(L-R), Fig. 3*B*) consistent with compensatory reflexes for perceived self-rotation. Translational optic flow elicited changes in the sum of left and right

wing stroke amplitudes (Δ(L+R), Fig. 3*C*), indicating symmetrical reactions consistent with an attempt to change total thrust. The responses to single visual features indicated a position-dependent attraction to the feature combined with velocity-dependent compensation for the feature's motion, consistent with classic models of stripe fixation in flies (Reichardt and Poggio 1976).

We did not observe any differences in the calcium response across different areas of the imaging region (data not shown). This is perhaps unsurprising, given that all the cells span the entire width of the fan-shaped body region we imaged. Rotational optic flow, whether composed of two or three stripes, elicited calcium responses for the duration of motion (Fig. 3*A*, second and third columns). Translational optic flow also excited the cells, and in this case their responses were phase locked to the stimulus motion (Fig. 3*A*, fourth column). Oscillation of one stripe resulted in a weaker response with some phase locking (Fig. 3*A*, leftmost column). The three peaks conspicuous in the responses to translational optic flow suggest that the cells respond to a stimulus parameter with three-fold periodicity. This pattern is informative, because these translational trials are divided into three periods of progressive (front-to-back) motion, separated by two periods of regressive motion. In contrast, the rotational stimuli always include a component of progressive motion (when features on one side move regressively, those on the other side move progressively). Thus, the periodicity of the responses appears to be correlated with the periodicity of progressive motion within each pattern of stimulus motion.

Because the responses to two or three stripes moving rotationally were not qualitatively different, we replaced the three stripes condition with an alternate trial type (Fig. 3, rightmost column). In this new trial type, the left and right stripes moved in anti-phase, but they started the trial moving regressively (contracting towards one another) instead of progressively. This pattern of motion resulted in three periods of regressive optic flow separated by two periods of progressive optic flow. We observed two prominent peaks in the responses to these trials (Fig. 3*A*, rightmost column), further suggesting that these cells selectively respond to progressive motion during flight.

ExFl1 neurons are excited by progressive and inhibited by regressive optic flow

The sensitivity to progressive optic flow during flight exhibited by ExFl1 neurons motivated a second set of imaging experiments using the improved calcium indicator GCaMP5 (Fig. 4*F*). In these experiments, we observed cellular responses to purely progressive or regressive optic flow, to test the idea that in flight these neurons are exclusively sensitive to the former. Simultaneously, we compared unilateral stimulation to bilateral stimulation, to determine if a simple summation occurs between responses to the two sides. There were 6 trial types in total. In two trials types, a single 18° wide dark stripe appeared with its rear edge directly in front of the fly, extending to either the left or right. After 1.5 s, this feature drifted progressively at 90° s^{-1} for one second, stopping with its rear edge 90° to the left or right. The stripe remained visible for 1.5 s and then disappeared. The third trial type combined these two stimuli, such that there were two progressively moving stripes. The remaining three trial types were the temporal reverse of the first three, with the features appearing in the lateral field of view and then drifting regressively to the center. The trials were presented in pseudorandom order and separated by 4 s.

Nine flies flew a minimum of 5 repetitions of each trial type and were included in our analysis (We required that they flew continuously from 0.5 s before the pattern appeared until 1 s after the pattern disappeared). We did not observe any differences between the responses to trials in which a single stripe was on the left or the right, so we combined them in Figure 4.

We again observed no systematic change from baseline fluorescence during trials in which the flies were not flying (Fig. 4*F*, black trace). During flight, however, progressively moving stimuli elicited reliable responses in these cells (Fig. 4*F*, blue line). When two stimuli were visible, the response was approximately twice as strong, suggesting an additive response to stimuli from each side. The neurons were unresponsive to the initial appearance of the visual features. They were also initially unresponsive to single regressively moving features, although they responded with a prolonged period of excitation at the cessation of regressive motion. These results for the initial parts of each trial type, up to the end of stimulus motion, corroborated our hypothesis of progressive motion sensitivity. Bilateral regressive optic

flow resulted in a moderate decrease in activity (Fig. 4*F*, rightmost column), however, and at the cessation of bilateral regressive motion the cells again displayed increased activity while the features remained visible. These aftereffects to unilateral and bilateral regressive motion cannot be explained by progressive motion sensitivity alone. It is tempting to suggest that they may be a response to the presence of visual features in the frontal field. However, identical features did not elicit responses when presented before motion in the progressive motion trials.

Whereas the response to bilateral progressive motion appears to be approximately a sum of the responses to unilateral progressive motion responses, a comparison of the responses to unilateral and bilateral regressive stimulation exposes a disparity. A simple summation of the responses to a single stripe moving regressively either on the left or the right side (Fig. 4*F*, third column) differs markedly from the response to the combined stimulus, i.e. two stripes moving regressively (Fig. 4*F*, right column). Bilateral regression appears to inhibit the cells, whereas a single regressive feature does not. In fact, the response to a single stripe begins to increase above baseline simultaneously with or even before the end of regressive motion. Because we do not have an estimate of the receptive field of these neurons, we cannot say whether this response is triggered purely by the offset of regressive motion or by a more complicated stimulus parameter. In any case, the nonlinearity between unilateral and bilateral stimulation indicates the existence of some bilateral comparison. Such a comparison could be useful in distinguishing translational from rotational motion.

Single cell electrophysiology supports the results of imaging experiments

The calcium imaging experiments described above identified reliable responses to progressive motion in the presynaptic terminal regions of the ExFl1 cells. However, because the terminals of approximately 14 cells overlap in the fan-shaped body, we could not distinguish responses of individual cells. Also, calcium imaging can only indicate changes over a limited dynamic range, and it is possible that the unresponsiveness we observed during quiescence was actually due to failure of GCaMP to detect activity changes (Jayaraman and Laurent 2007). To address these questions, we used whole-cell patch-clamp

electrophysiology to record from the somata of individual GFP-positive neurons. Like nearly all insect neurons, the somata of ExFl1 neurons are located in a cortex on the outer surface of the brain. Because of their frontal location (superior to the antennal lobes), these recordings required that the head of the animal be positioned such that the eyes were partially occluded by the mounting stage. During each recording we filled the cell with Biocytin and subsequently confirmed that the cells we recorded from were indeed GFP-positive (Fig. 1*C*). In these electrophysiology experiments, the stimuli were similar to the drifting patterns described above, except that the LEDs were green, the display was slightly shifted to the right to accommodate recording equipment, and the trials were separated by only 2 s. We recorded from seven animals (one cell in each) that flew for at least four trials of each type. We still required that flies flew for at least 0.5 s before the pattern appeared and the entire time it was visible, but we relaxed the condition on flying after the pattern disappeared.

Unlike visual interneurons in the optic lobes that have been recorded from previously (Joesch et al. 2010; Maimon et al. 2010; Schnell et al. 2010), these cells regularly fire action potentials (Fig. 4*C*). We recorded a membrane potential of 49 ± 5.3 mV and a resting spike rate of 4.3 ± 1.5 Hz (mean ± std). The mean spike rate of every cell increased modestly during flight (5.1 ± 1.7 Hz; Fig. 2*A*) ($p=.0018$, $t=-5.30$, two-tailed paired t-test). The animals again displayed robust behavioral responses to the movement of the patterns.

As expected from our calcium imaging experiments, during quiescence the cells showed negligible responses to visual stimuli (Fig. 4*G*, black line). During flight, they did respond to progressive optic flow with increases in spike rate (Fig 4*G*, blue line). In order to quantify these observations, we divided the trials into three periods: half a second before the pattern appeared, one second during which the pattern was in motion, and one second after the pattern stopped moving. We compared the spike rates during the latter two periods for each trial type to the spike rate during the first period. Responses to single stripes were somewhat variable between cells and between trials of the same cell (Fig. 4*B,C*), but were not consistently confined to motion in either the ipsi- or contralateral visual field. Therefore, we pooled

responses to a single stripe as in the calcium imaging experiments. For trials with one stripe moving progressively, the mean spike rate increased from 4.6 ± 1.9 Hz before the stripe appeared to 5.8 ± 1.4 Hz during its motion (p=.0086, t=-3.84, two-tailed paired t-test, Fig. 4*G*, left column). In trials with two stripes moving progressively, the mean spike rate increased from 4.5 ± 1.9 Hz to 6.0 ± 2.0 Hz (p=.0226, t=-3.05, two-tailed paired t-test) and remained above baseline (spike rate 5.5 ± 1.3 Hz) in the second after motion (p=.0300, t=-2.83, two-tailed paired t-test, Fig. 4*G*, second column).

We also observed responses at the end of regressive motion stimuli, corroborating the observations of the second set of imaging experiments. In trials in which one stripe moved regressively, the mean spike rate after motion was 5.9 ± 1.5 Hz, compared to 4.8 ± 2.0 Hz before the stripe appeared (p=.0452, t=-2.52, two-tailed paired t-test). The average spike rate during motion showed an insignificant increase to 5.3 ± 1.5 Hz (p=.1661, t=-1.58, two-tailed paired t-test), qualitatively similar to the calcium response (Fig. 4*F* third column). After two stripes ceased moving regressively, the mean spike rate was 5.7 ± 1.8 Hz, significantly higher than the 3.9 ± 1.5 Hz we observed before the stripes appeared (p=.0028, t=-4.88, two-tailed paired t-test, Fig. 4*G*, rightmost column). Again, there is a rough similarity between the changes in spike rate in response to this stimulus and the corresponding calcium responses (Fig. 4*F* rightmost column).

During quiescence, the largest effects we observed during these periods were an increase in spike rate from 3.9 ± 1.6 Hz to 4.9 ± 1.6 Hz and 4.4 ± 1.5 Hz during and after regressive motion by two stripes (p=.0091, t=-3.78, and .0212, t=-3.10, respectively, two-tailed paired t-test). After these comparisons, neither period in any trial type were significantly different from that trial's baseline with $p < .0535$ by two-tailed paired t-test. The low-pass filtered membrane potential of these neurons appeared to follow the same general form as their spike rate in response to these stimuli, but none of the periods approached the significant responses we observed in spike rate (data not shown).

The changes in spike rate that we observed in response to the visual stimuli were more variable and subtle than the results using GCaMP imaging. There are several possible explanations for this quantitative

discrepancy. First, the physical infrastructure required for our patch recordings partially obstructed the view of both compound eyes, and thus the extent of the visual stimulus was smaller and more restricted to the ventral visual field. For this reason, the stimuli in our electrophysiology experiments may have been weaker. Second, whole cell patch recording is more invasive than imaging because it requires disrupting the neurolemma surrounding the brain, which might change the extracellular milieu, and the cell is perfused with intracellular solution, which may further alter its physiology. Third, whereas imaging experiments record the summed responses of the entire ExFl1 population targeted in the Gal4 line, our patch recordings sample one cell at a time. If there are differences among cells within this population, we may simply have failed to sample a cell with a particularly strong response to the visual stimuli. In support of this possibility, a recent study reported high levels of variability to visual stimuli in tangential neurons of the fan-shaped body in locusts, suggesting that such variability may be typical of central complex neurons (Rosner and Homberg 2013). Fourth, there might be a non-linear relationship between spike rate and intracellular calcium levels such that even a modest increase in the spike frequency of individual cells could generate the responses we observed in imaging experiments when summed across the entire population of ExFl1 neurons. Finally, spike rate might not be the most relevant feature of the neuronal response. Local subthreshold membrane potential fluctuations that are not visible in recordings from the cell body might be sufficient to activate calcium currents or the release of calcium from internal stores. Despite these caveats, the data obtained from single cell recordings, though subtle, nevertheless qualitatively support the observation of progressive motion sensitivity during flight in the ExFl1 neurons based on imaging. Moreover, because we imaged a known presynaptic region, it is probable that calcium responses we observed in the terminals trigger synaptic release and are thus physiologically relevant to downstream neurons.

Responses to prolonged global optic flow resemble responses to simple stripe patterns

In the experiments described above, we tested for visual responses in ExFl1 neurons using sets of horizontally moving vertical stripes to create simple patterns of translational and rotational optic flow.

364 The cells were excited by front-to-back motion, which crudely approximates the optic flow an animal
365 experiences during forward locomotion, as well as the cessation of back-to-front motion. Two caveats
366 with these stimuli, however, are that they include the appearance, disappearance, and movement of
367 distinct objects (the stripes) and the periods of translational optic flow were relatively brief. To address
368 these shortcomings, we created more complex stimuli in which translation was simulated using a field of
369 bright points randomly arranged in 3 dimensions. The pattern was created assuming that the fly was
370 moving forward or backward at 1 m s^{-1} for 4 s through a virtual space consisting of point-like objects
371 whose retinal size never changed (< 2° wide). On average there were 20 points per cubic meter, and the
372 fly could only see the points that were less than 2 m away. Three successive frames of such a stimulus are
373 shown in Fig. 5*A*. Before and after each motion trial, we held the pattern stationary. Although the pattern
374 did not simulate all aspects of real optic flow, the distribution of retinal speed over the visual field did
375 approximate a more naturalistic pattern of image motion during forward and backward translation. In
376 addition, these patterns completely lacked the prominent edges of highly correlated luminance changes
377 present in previous experiments.

378 Using this 'star field' pattern, we tested 13 flies, each of which flew for a minimum of 739 s while we
379 imaged neuronal activity using GCaMP5. In response to simulated progressive motion, we again observed
380 excitation in the ExFl1 neurons during flight (Fig. 5*B*, left column). This excitation diminished to baseline
381 levels after several seconds. In response to regressive motion we observed a prominent decrease in
382 activity, which persisted for the entire 4 s trial duration followed by a large rebound in excitation at the
383 end of stimulus motion (Fig. 5*B*, right column). The neurons were relatively inactive while the flies were
384 not flying, although they did exhibit very small but consistent responses opposite to those during flight
385 (decrease to progressive motion, increase to regressive motion). These observations are generally
386 consistent with those presented in Fig. 4, confirming that in flight these cells respond with increased
387 activity to progressive optic flow, decreased activity to regressive optic flow, and increased activity to the
388 cessation of regressive optic flow. Further, these results demonstrate that the responses are not limited to

motion of salient visual objects, but can be elicited by patterns of image motion using a large array of fine points.

Neuronal responses are not correlated with variability in wing motor behavior

Our analysis thus far has implicitly assumed that ExFl1 neurons are members of a visual pathway. However, given the putative role of the central complex in regulating motor actions, it is possible that the changes in ExFl1 neuron activity we recorded were more directly related to the changes in behavior elicited by our visual stimuli. If this were the case, we would expect that the neuronal responses in each trial would be highly correlated with the behavioral changes. To look for such a correlation, we exploited the variability in the behavioral responses of flies to the star field stimuli. In some trials, the animals responded to the visual stimulus with large changes in L+R, whereas in others they were comparatively unresponsive. We computed the mean $\Delta F/F$ and L+R from one to two seconds after the stimulus started moving in each trial (Fig. 5*B,C* dark gray background). For each of the 13 flies, we computed a linear regression[1] between these individual trial responses separately for trials with progressive and regressive optic flow (Fig. 5*E*). We expected a negative correlation, because progressive optic flow elicits increases in $\Delta F/F$ and decreases in L+R. Out of these 26 linear regressions, we found 3 cases in which the slopes were significantly different from zero at the $p<.05$ level (all three of which were negative). However, only one case was significantly different from zero after correcting for multiple comparisons using the false discovery rate procedure. For this regression (shown in black in Fig. 5*E*), the r^2 value was 0.38, the p-value was 0.0017, and the slope was -0.054 degrees^{-1}. It is possible that a correlation with motor output would be more apparent if short term changes in the responses were compared. For this reason, we conducted the same analysis after first subtracting the mean values of $\Delta F/F$ and L+R during a 0.5 s period prior to stimulus motion (thereby performing a baseline subtraction of the two signals). Using this approach, we found one set of progressive trials from one fly (but not one of the three identified in the previous analysis) that showed a correlation significantly different from zero at $p<.05$ (slope = -0.055 degrees^{-1}), but it did not pass the false discovery rate procedure. We also repeated this analysis

using turning behavior (L-R), instead of the thrust response (L+R), but again found only one case of significant correlation out of 26, which did not survive the false discovery rate procedure. These results clearly indicate that the magnitude of ExFl1 neuron activity is not strongly correlated with variability in the wing motor responses we recorded. Although it is probable that these cells contribute to modulating flight behavior, their responses are better correlated with visual input.

DISCUSSION

We recorded the responses of a class of wide-field fan-shaped body (ExFl1) neurons during flight and quiescence. Using two-photon excitation of the genetically encoded calcium indicator GCaMP3, we observed increased activity in the presynaptic (output) region of these cells with the onset of flight (Fig. 2) and in response to progressively moving visual patterns during flight (Fig. 3). During quiescence the cells were unresponsive to the presented visual stimuli. We tested further the cellular responses using GCaMP5 (Figs. 4 and 5) and whole-cell patch-clamp recordings (Fig. 4) with patterns of purely progressive or regressive motion, confirming progressive motion sensitivity, and indicating additional prolonged responses after regressive motion.

Fan-shaped body neurons in flies

Our observation of flight-dependent visual responses indicates that the ExFl1 neurons must minimally receive input (direct or indirect) from two sets of cells, one sensitive to visual motion and one conveying information about whether or not the animal is flying. Their dendritic branches in the inferior medial protocerebrum and the ventral bodies make it likely that they receive many different types of input. The electrophysiology experiments suggest that single cells might receive input from both visual hemispheres, although they are not conclusive because of high variability in the responses. Unfortunately, little is known of the types of information represented in these two regions and further study will be required to determine the identities of cells presynaptic to the ExFl1 neurons.

There is a larger body of work concerning the fan-shaped body, where ExFl1 cells have output terminals. Although it would be premature to hypothesize the precise identities of downstream neurons, a few general observations are possible. Based on anatomical data, it has been proposed that the fan-shaped body (and the central complex at large) possesses a stereotyped organization composed of large-field input fibers spanning horizontal layers and output fibers arranged in small-field vertical columns (Hanesch et al. 1989; Young and Armstrong 2010). The ExFl1 neurons clearly fit in this architecture as an input element. Each ExFl1 neuron spans the entire width of the fan-shaped body. If azimuth is encoded in columnar order, this anatomy would suggest that there should be no retinotopic representation in these cells, which is consistent with our observations.

Similar input cell classes have been anatomically defined for over 20 years. Hanesch et al. (1989) described two types of large-field neurons in the fan-shaped body, those whose fibers traverse the median canal of the ellipsoid body (termed Fm, for median), and those whose fibers take a lateral route, the Fl neurons. Those authors remarked that the latter (of which the ExFl1 neurons are a subset) are heterogeneous and can be found in all layers of the fan-shaped body. In addition to the ExFl1 neurons, another subset of Fl neurons (ExFl2 cells) has been studied. These cells arborize in layer 5 of the fan-shaped body, dorsal to the ExFl1 neurons. Both ExFl1 and ExFl2 neurons have been implicated in visual memory formation (Liu et al. 2006; Wang et al. 2008) and it is possible that they convey different aspects of visual information to the fan-shaped body during flight. Phillips-Portillo (2012) recorded intracellularly from dorsally arborizing fan-shaped body cells in the flesh fly, similar to the ExFl2 neurons in *Drosophila* (see also Phillips-Portillo and Strausfeld 2012). These cells fire action potentials at a rate between 5 and 15 Hz in quiescent flies. He observed no responses to a variety of visual and mechanical stimuli, except in one cell, which responded to air puffs and flashes of light in the dorsal field of view. Their activity did not appear to change when animals walked on a Styrofoam ball, although the sample size was limited (J. Phillips-Portillo, personal communication). Given our results it is reasonable to propose that the general lack of responsiveness reported in this prior study was due to the inability of the animals to fly during

recordings. One cell type possibly postsynaptic to the ExFl1 cells are the so-called pontine neurons that connect the dorsal and ventral layers of a single fan-shaped body column. Phillips-Portillo (2012) recorded from these cells as well, and observed variable responses to changes in illumination and directional selectivity to moving visual objects in agreement with a role of the fan-shaped body in visual navigation.

Fan-shaped body functional anatomy

Perhaps the most detailed account of the functional anatomy of the central complex has been made in the desert locust *Schistocerca gregaria*. Researchers working with this species have focused on the central complex as the site of analysis of celestial polarization information. They have identified large numbers of cells that respond to polarized light in the ellipsoid body and the protocerebral bridge, among other regions. However, there is a marked lack of polarization sensitive cells in the fan-shaped body (Vitzthum et al. 2002), although this region receives input from visual areas (Homberg 2004). Variable responses to polarized light from several types of fan-shaped body columnar neurons have been reported (Vitzthum et al. 2002; Heinze and Homberg 2008, 2009). Recently, neurons in the fan-shaped body and other parts of the locust central complex have been reported to respond to translating and expanding visual stimuli, supporting a role in visual control of behavior by this brain region (Rosner and Homberg 2013). Candidates for synaptic partners of ExFl1 responsive to flight can be found in the locust literature. The columnar neurons CPU increase activity during flight (Homberg 1994) and conceivably receive input from neurons similar to the ExFl1 neurons (El Jundi et al. 2009).

Fan-shaped body neuronal responses during locomotion

Our results suggest that the fan-shaped body plays a role in visual processing during flight. One type of visual stimulation that the ExFl1 cells respond to, progressive and regressive optic flow, is experienced when an animal moves forward or backward through the environment. This observation suggests that these neurons might be suited to tasks such as estimating flight speed or measuring forward progress. The aftereffect of increased activity following the cessation of regressive motion (right two columns of Fig.

4*F,G* and Fig. 5*B*) is a peculiar feature. Perhaps there is some additional sensitivity to front-to-back acceleration which is triggered by the end of regressive motion, or the cessation of unilateral regressive motion in the receptive field of these cells is itself excitatory. In addition, unilateral and bilateral regressive motion appear to influence the cells differently, suggesting that some comparison between the two sides is taking place. More work is required to explain these phenomena.

The fan-shaped body has been implicated in a variety of behaviors. There have been numerous studies based on genetic intervention in the central complex which are not immediately reconcilable with our data. Mutations that affect the structure of the central complex result in deficits in walking (Strauss and Heisenberg 1993), expressing tetanus toxin in large-field fan-shaped body neurons results in decreased total walking activity (Martin et al. 1999), and the action of various peptides in the fan-shaped body influences locomotor activity (Kahsai et al. 2010). Liu et al. (2006) reported that ExFl1 neurons are involved in memory of an object's orientation (see also Li et al. 2009). In this Discussion we focus on studies that report the electrophysiology of cells, albeit from other species. In *Drosophila*, more work is necessary before a complete explanation of the role of the fan-shaped body is possible.

Research in the cockroach *Balberus discoidalis* has focused on the function of the central complex during locomotion. Researchers have recorded from fan-shaped body neurons while the animal walks in place on a greased platform or a Styrofoam ball. In this preparation, some neurons in the central complex change their firing rates prior to turns and changes in step frequency (Bender et al. 2010; Guo and Ritzmann 2013). Of particular interest with respect to this study is an observation of neurons in the central complex that respond to antennal stimulation while the animal is quiescent, but do not respond to the same stimulation while the animal is walking. Bender and co-workers recorded from 15 neurons in the fan-shaped body, eight of which were responsive to tactile stimuli while the animal was standing still. Of these, only one responded while the animal was walking in a tethered preparation. Although the effect of active locomotion is opposite to our findings (reducing instead of educing responses to sensory stimuli), these results lend support to the idea that the fan-shaped body is involved in gating relevant stimuli based

on locomotor state. The ability to filter out irrelevant sensory information and focus on behaviorally relevant features is likely a general feature of nervous systems (Cherry 1954; Knudsen 2007). In this study we observed activity-gated visual responses in one small set of neurons in the fan-shaped body. As more cell types are characterized, our understanding of the computations performed by the central complex will grow, hopefully leading to an explanation of the role played by this fascinating structure in generating organismal behavior.

REFERENCES

Akerboom J, Chen T-W, Wardill TJ, Tian L, Marvin JS, Mutlu S, Calderón NC, Esposti F, Borghuis BG, Sun XR, Gordus A, Orger MB, Portugues R, Engert F, Macklin JJ, Filosa A, Aggarwal A, Kerr R a, Takagi R, Kracun S, Shigetomi E, Khakh BS, Baier H, Lagnado L, Wang SS-H, Bargmann CI, Kimmel BE, Jayaraman V, Svoboda K, Kim DS, Schreiter ER, Looger LL. Optimization of a GCaMP calcium indicator for neural activity imaging. *J Neurosci* 32: 13819–40, 2012.

Bahl A, Ammer G, Schilling T, Borst A. Object tracking in motion-blind flies. *Nat Neurosci* 16: 730–8, 2013.

Baird E, Srinivasan M V, Zhang S, Cowling A. Visual control of flight speed in honeybees. *J Exp Biol* 208: 3895–905, 2005.

Bender JA, Dickinson MH. Visual stimulation of saccades in magnetically tethered *Drosophila*. *J Exp Biol* 209: 3170–82, 2006.

Bender JA, Pollack AJ, Ritzmann RE. Neural activity in the central complex of the insect brain is linked to locomotor changes. *Curr Biol* 20: 921–6, 2010.

Card G, Dickinson MH. Visually mediated motor planning in the escape response of *Drosophila*. *Curr Biol* 18: 1300–7, 2008.

Cherry EC. Some further experiments upon the recognition of speech, with one and with two ears. *J Acoust Soc Am* 26: 554, 1954.

Chiappe ME, Seelig JD, Reiser MB, Jayaraman V. Walking modulates speed sensitivity in *Drosophila* motion vision. *Curr Biol* 20: 1470–5, 2010.

Clark DA, Bursztyn L, Horowitz MA, Schnitzer MJ, Clandinin TR. Defining the computational structure of the motion detector in *Drosophila*. *Neuron* 70: 1165–77, 2011.

Fry SN, Rohrseitz N, Straw AD, Dickinson MH. Visual control of flight speed in *Drosophila melanogaster*. *J Exp Biol* 212: 1120–30, 2009.

Gibson JJ. Visually controlled locomotion and visual orientation in animals. *Brit J Psychol* 49: 182–94, 1958.

Götz K. Course-control, metabolism and wing interference during ultralong tethered flight in *Drosophila melanogaster*. *J Exp Biol* 128: 35–46, 1987.

Guo P, Ritzmann RE. Neural activity in the central complex of the cockroach brain is linked to turning behaviors. *J Exp Biol* 216: 992–1002, 2013.

Hammond S, O'Shea M. Escape flight initiation in the fly. *J Comp Physiol A* 193: 471–6, 2007.

Hanesch U, Fischbach K, Heisenberg M. Neuronal architecture of the central complex in Drosophila melanogaster. *Cell Tissue Res.* .

Heinze S, Homberg U. Neuroarchitecture of the central complex of the desert locust: Intrinsic and columnar neurons. *J Comp Neurol* 511: 454–78, 2008.

Heinze S, Homberg U. Linking the input to the output: new sets of neurons complement the polarization vision network in the locust central complex. *J Neurosci* 29: 4911–21, 2009.

Homberg U. Flight-correlated activity changes in neurons of the lateral accessory lobes in the brain of the locust *Schistocerca gregaria*. *J Comp Physiol A* 175: 597–610, 1994.

Homberg U. In search of the sky compass in the insect brain. *Die Naturwissenschaften* 91: 199–208, 2004.

Jayaraman V, Laurent G. Evaluating a genetically encoded optical sensor of neural activity using electrophysiology in intact adult fruit flies. *Front Neural Circuits* 1: 3, 2007.

Joesch M, Schnell B, Raghu SV, Reiff DF, Borst A. ON and OFF pathways in *Drosophila* motion vision. *Nature* 468: 300–4, 2010.

El Jundi B, Heinze S, Lenschow C, Kurylas A, Rohlfing T, Homberg U. The locust standard brain: a 3D standard of the central complex as a platform for neural network analysis. *Front Syst Neurosci* 3: 21, 2009.

Jung SN, Borst A, Haag J. Flight activity alters velocity tuning of fly motion-sensitive neurons. *J Neurosci* 31: 9231–7, 2011.

Kahsai L, Martin J-R, Winther AME. Neuropeptides in the *Drosophila* central complex in modulation of locomotor behavior. *J Exp Biol* 213: 2256–65, 2010.

Knudsen EI. Fundamental components of attention. *Annu Rev Neurosci* 30: 57–78, 2007.

Koenderink JJ. Optic flow. *Vis Res* 26: 161–179, 1986.

Li W, Pan Y, Wang Z, Gong H, Gong Z, Liu L. Morphological characterization of single fan-shaped body neurons in *Drosophila melanogaster*. *Cell Tissue Res* 336: 509–19, 2009.

Liu G, Seiler H, Wen A, Zars T, Ito K, Wolf R, Heisenberg M, Liu L. Distinct memory traces for two visual features in the *Drosophila* brain. *Nature* 439: 551–556, 2006.

Loesel R, Nässel DR, Strausfeld NJ. Common design in a unique midline neuropil in the brains of arthropods. *Arth Struct & Dev* 31: 77–91, 2002.

Maimon G, Straw AD, Dickinson MH. Active flight increases the gain of visual motion processing in *Drosophila*. *Nat Neurosci* 13: 393–9, 2010.

Martin JR, Raabe T, Heisenberg M. Central complex substructures are required for the maintenance of locomotor activity in Drosophila melanogaster. *J Comp Physiol A* 185: 277–88, 1999.

583 **Paulk A, Millard SS, van Swinderen B**. Vision in *Drosophila*: seeing the world through a model's eyes.
584 *Annu Rev Entomol* 58: 313–32, 2013.

585 **Phillips-Portillo J, Strausfeld NJ**. Representation of the brain's superior protocerebrum of the flesh fly,
586 *Neobellieria bullata*, in the central body. *J Comp Neurol* 520: 3070–87, 2012.

587 **Phillips-Portillo J**. The central complex of the flesh fly, *Neobellieria bullata*: recordings and
588 morphologies of protocerebral inputs and small-field neurons. *J Comp Neurol* 520: 3088–104, 2012.

589 **Reichardt W, Poggio T**. Visual control of orientation behaviour in the fly. *Q Rev Biophys* 9: 311–375,
590 1976.

591 **Rosner R, Homberg U**. Widespread sensitivity to looming stimuli and small moving objects in the
592 central complex of an insect brain. *J Neurosci* 33: 8122–33, 2013.

593 **Schnell B, Joesch M, Forstner F, Raghu S V, Otsuna H, Ito K, Borst A, Reiff DF**. Processing of
594 horizontal optic flow in three visual interneurons of the *Drosophila* brain. *J Neurophysiol* 103: 1646–57,
595 2010.

596 **Seelig J, Chiappe M, Lott G, Dutta A**. Two-photon calcium imaging from head-fixed *Drosophila*
597 during optomotor walking behavior. *Nature* 7: 535–540, 2010.

598 **Srinivasan M, Zhang S, Bidwell N**. Visually mediated odometry in honeybees. *J Exp Biol* 200: 2513–
599 22, 1997.

600 **Strausfeld NJ, Hirth F**. Deep homology of arthropod central complex and vertebrate basal ganglia.
601 *Science* 340: 157–161, 2013.

602 **Strauss R, Heisenberg M**. A higher control center of locomotor behavior in the *Drosophila* brain. *J*
603 *Neurosci* 13: 1852–61, 1993.

604 **Suver MP, Mamiya A, Dickinson MH**. Octopamine neurons mediate flight-induced modulation of
605 visual processing in *Drosophila*. *Curr Biol* 22: 2294–302, 2012.

606 **Tian L, Hires SA, Mao T, Huber D, Chiappe ME, Chalasani SH, Petreanu L, Akerboom J,**
607 **McKinney S a, Schreiter ER, Bargmann CI, Jayaraman V, Svoboda K, Looger LL**. Imaging neural
608 activity in worms, flies and mice with improved GCaMP calcium indicators. *Nat Methods* 6: 875–81,
609 2009.

610 **Vitzthum H, Muller M, Homberg U**. Neurons of the central complex of the locust *Schistocerca*
611 *gregaria* are sensitive to polarized light. *J Neurosci* 22: 1114–25, 2002.

612 **Wang Z, Pan Y, Li W, Jiang H, Chatzimanolis L, Chang J, Gong Z, Liu L**. Visual pattern memory
613 requires foraging function in the central complex of *Drosophila*. *Learn Mem* 15: 133–42, 2008.

614 **Young JM, Armstrong JD**. Structure of the adult central complex in *Drosophila*: organization of distinct
615 neuronal subsets. *J Comp Neurol* 518: 1500–24, 2010.

616

FIGURE CAPTIONS

Figure 1.

Calcium imaging in ExFl1 neurons during flight and quiescence. *A*, Schematic of the recording apparatus. The objective of the two-photon microscope accessed the fly from above. Below, the fly viewed an LED display. *B*, An example frame from the camera monitoring the fly's behavior. Superimposed are lines depicting the instantaneous estimates of left (L) and right (R) wing stroke amplitudes, measured increasing from the posterior body axis, defined as -90°. *C*, Maximum intensity projection through a depth of 67.5 µm of a coronal view of GFP expression (green) in the NP6510 driver line and a single Biocytin-filled ExFl1 cell (magenta). Dorsal direction is toward the top of the page, scale bar 50 µm. *D*, The mean of all 22,100 frames acquired during an experiment. We defined the region of interest (ROI) as the brightest 960 pixels (90^{th} percentile), outlined in red, and the background as the dimmest 960 pixels (10^{th} percentile), outlined in cyan. Scale bar 25 µm. *E*-*G*, Example data from one fly of all trials of one trial type with the mean over all trials plotted in heavy lines. *E*, The sum of ROI fluorescence during flight is plotted in blue and the background fluorescence during flight is in cyan. The ROI during quiescence is in black and background during quiescence is in green (almost indistinguishable from flight trial data). *F*, Right wing stroke amplitude subtracted from left wing stroke amplitude (positive deflections indicate an attempted turn to the right). *G*, Sum of left and right wing stroke amplitudes (increases indicate increasing thrust). *H*, Schematic of stimuli. The azimuthal position and width of the visual features are indicated by vertical position and width of the dark patches, respectively, for each time point. Increases (decreases) denote rightward (leftward) direction. Two vertical stripes appeared at time t=0 s at +45° and -45° and moved toward the center. Their horizontal positions oscillated through two full cycles, then both disappeared at time t=4 s. *I*, Schematic of stimuli. Two dark 18°-wide stripes were presented on a blue background and centered at +45° (right) from midline and -45° (left) of midline. The stimulus array spanned from -108° to +108° in azimuth and 32° above and below the horizontal axis of the fly's head in elevation.

Figure 2.

ExFl1 neuronal activity increases during flight. *A*-*B*, Data in the left and right column are aligned to the time of flight initiation and cessation, respectively. Lines represent the mean of individual fly responses and shaded areas indicate the upper and lower quartiles. The mean responses of seven flies expressing GCaMP3 are plotted in blue, 21 flies expressing GCaMP5 in black, eight GFP-expressing flies in green, and seven patch-clamp flies in magenta (spike rate computed using a sliding Gaussian window with 75 ms standard deviation). To be included a fly had to both start and stop flying at least once during a recording. Data were taken from the same experiments as reported in later figures. *A*, Using both calcium indicators and electrophysiology we observed an increase in activity accompanying flight onset. Activity remained above baseline, decreasing after the animal stopped flying. GFP controls showed no change in fluorescence, indicating no artifact due to brain motion. *B*, Summed left and right wing stroke amplitudes for all conditions.

Figure 3.

Responses to oscillating visual stimuli during flight and quiescence. *A*-*C*, Mean of 12 individual fly responses are depicted in lines, shaded areas indicate upper and lower quartiles. Trials in which the animals were flying are in blue, quiescent trials are in black. In the first column only a single stripe was present, which is ambiguous with respect to rotation and translation. In the second and third columns are data from rotational stimuli, in which features moved in the same direction. The rightmost two columns contain data from trials with translational stimuli, in which features moved mirror symmetrically about the midline. Each fly participated in four trial types, the first, second, and fourth columns, and either the third column (five flies) or the fifth column (seven flies). *A*, During flight, $\Delta F/F$ increased in response to all visual stimuli, and was phase-locked to translational stimulus motion. *B*, Change in turning response (difference between left and right wing stroke amplitudes). We subtracted the mean during the 0.5 s preceding each trial. Rotational motion elicited attempted turns in the same direction by the flies. *C*,

Change in summed wing stroke amplitudes. Flies responded to expanding (contracting) stimuli with decreases (increases) in wing stroke amplitudes. We subtracted the mean in the 0.5 s preceding each trial. *D*, Schematic of stimuli. The azimuthal position and width of the visual features are indicated by vertical position and width of the dark patches, respectively, for each time point. Increases (decreases) denote rightward (leftward) direction. In the left column, one vertical stripe appeared at time t=0 s at +45° (right) and moved to the right. Its horizontal position oscillated through two full cycles, then it disappeared at time t=4 s.

Figure 4.

Responses to drifting progressive and regressive stimuli during flight and quiescence. *A*-*E*, Patch-clamp data from a single fly. *A*, Example membrane potential during a progressive motion one-stripe trial. *B*-*C*, Spike rasters showing data from all progressive one-stripe trials (flight trials in *B*, quiescent trials in *C*). *D*, Mean spike rate during flight (blue) and quiescence (black) for data in *B* and *C*, computed using a sliding Gaussian window with 75 ms standard deviation. *E*, Same as Figure 3*D*. *F*, Mean responses of nine flies expressing GCaMP5 in ExFl1 cells during flight in blue and quiescence in black. Shaded areas indicate upper and lower quartiles. Regressive motion stimuli (right two columns) resulted in activity after stimulus motion that cannot be accounted for by progressive motion sensitivity. *G*, Mean instantaneous spike frequency computed as in *D* for seven flies. Increases during progressive motion (left two columns) and after regressive motion (right two columns) were consistent with imaging data, although small in magnitude. *H*, similar to Figure 3*D*.

Figure 5.

Responses to global patterns of optic flow. We simulated four seconds of forward (progressive) and backward (regressive) motion through a cloud of point-like objects (‘star field’). *A*, Three frames from the

stimulus simulating progressive motion. Lit pixels in the first frame are indicated in dark gray, lit pixels 100 ms later are light gray, lit pixels 200 ms after the first frame are white. *B* and *C*, Mean responses of 13 flies, upper and lower quartiles indicated by shaded areas. Light gray background indicates periods of stimulus motion. *B*, GCaMP5 fluorescence in ExFl1 neurons increased in response to progressive motion and decreased in response to regressive motion while the animal was in flight (blue). Changes during quiescence were negligible (black). *C*, Summed wing stroke amplitude decreased during progressive motion and increased during regressive motion. *D*, Simulated velocity through the 'star field.' *E*, Summed wing stroke amplitude is not correlated with ΔF/F on a trial-by-trial basis. For each fly we calculated the mean ΔF/F and L+R from 1 to 2 s after the onset of stimulus motion (dark gray background in *B*-*D*) in each trial. Each point represents a single trial and each fly is represented by a single color. Data from progressive trials are on the left, regressive trials are on the right. Only the progressive trials from one fly (data in black) revealed a statistically significant relationship between ΔF/F and L+R, indicated by the black linear regression line.

FOOTNOTES

[1] Although the wing stroke responses are measured as an angle, they are sufficiently tightly grouped to justify using linear regression on circular data.

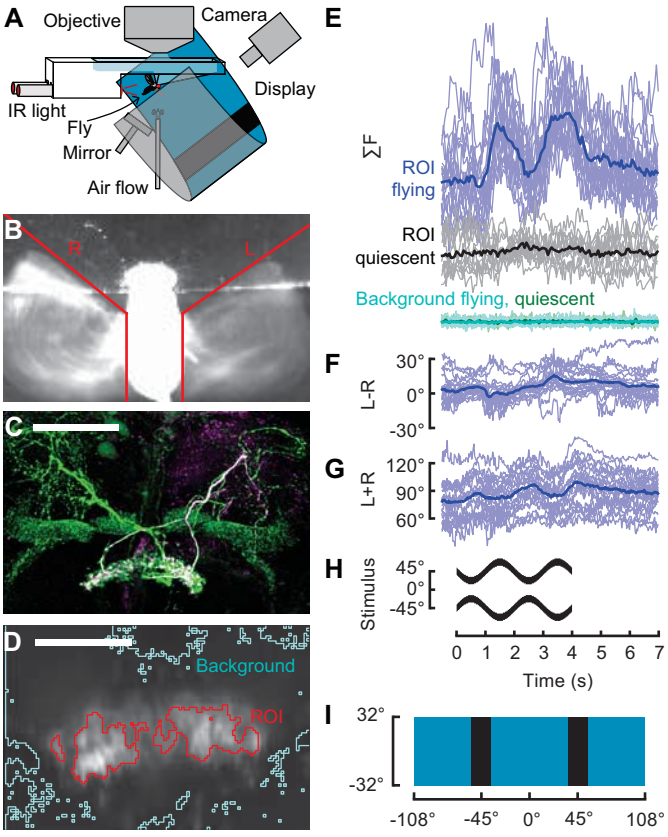
A
Objective
Camera
Display
IR light
Fly
Mirror
Air flow
B
R
L
C
D
Background
ROI
E
∑F
ROI
flying
ROI
quiescent
Background flying, quiescent
F
L-R
30°
0°
-30°
G
L+R
120°
90°
60°
H
Stimulus
45°
0°
-45°
0 1 2 3 4 5 6 7
Time (s)
I
32°
-32°
-108° -45° 0° 45° 108°

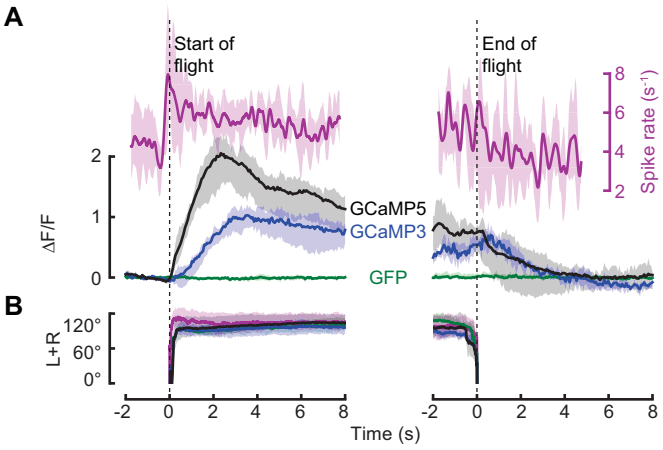
A
Start of flight
End of flight
Spike rate (s⁻¹)
8
6
4
2
ΔF/F
2
1
0
GCaMP5
GCaMP3
GFP
B
L+R
120°
60°
0°
-2
0
2
4
6
8
Time (s)

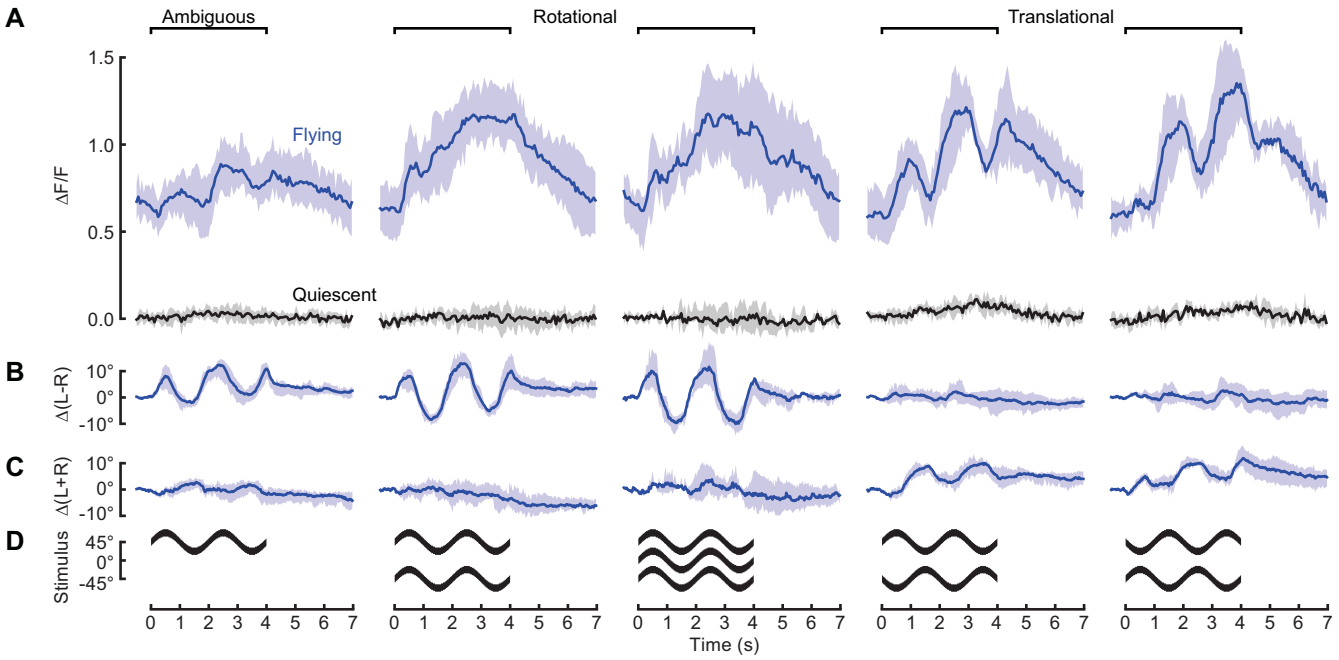
A
Ambiguous
Rotational
Translational
1.5
1.0
0.5
0.0
ΔF/F
Flying
Quiescent
B
Δ(L-R)
10°
0°
-10°
C
Δ(L+R)
10°
0°
-10°
D
Stimulus
45°
0°
-45°
0 1 2 3 4 5 6 7
Time (s)

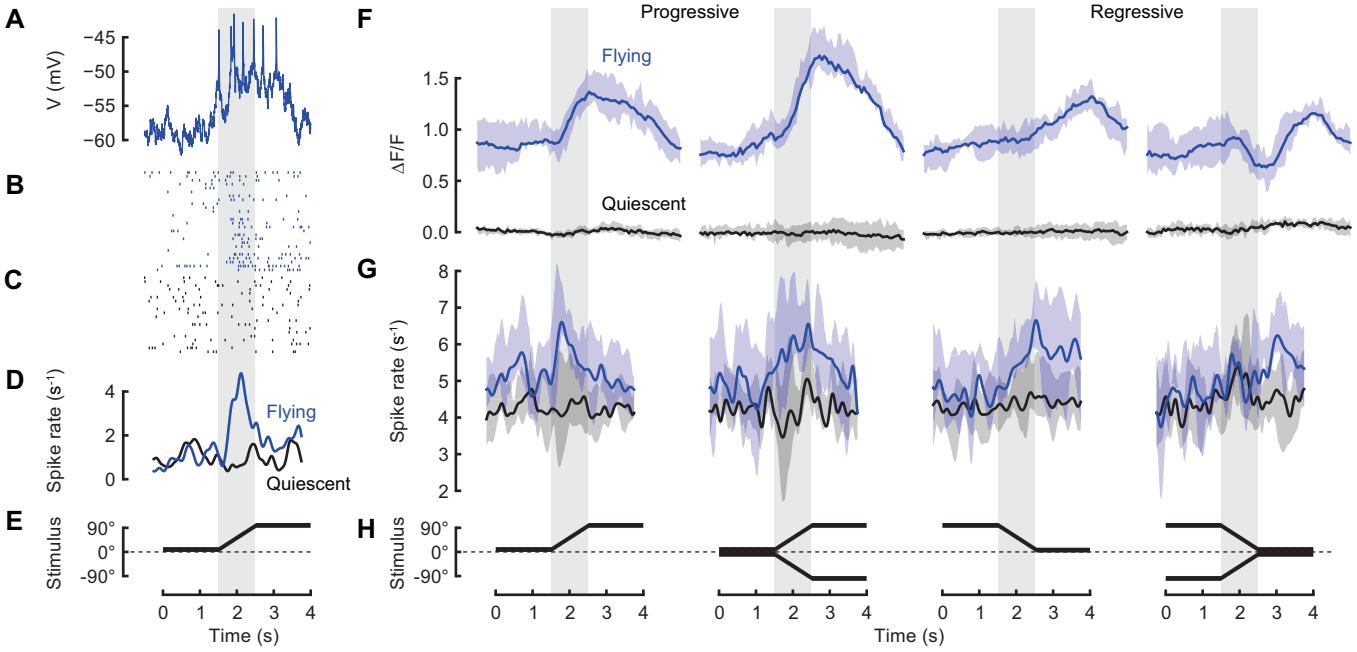
A
V (mV)
−45
−50
−55
−60
B
C
D
Spike rate (s⁻¹)
4
2
0
Flying
Quiescent
E
Stimulus
90°
0°
-90°
0 1 2 3 4
Time (s)
F
Progressive
Regressive
Flying
Quiescent
ΔF/F
1.5
1.0
0.5
0.0
G
Spike rate (s⁻¹)
8
7
6
5
4
3
2
H
Stimulus
90°
0°
-90°
0 1 2 3 4
Time (s)

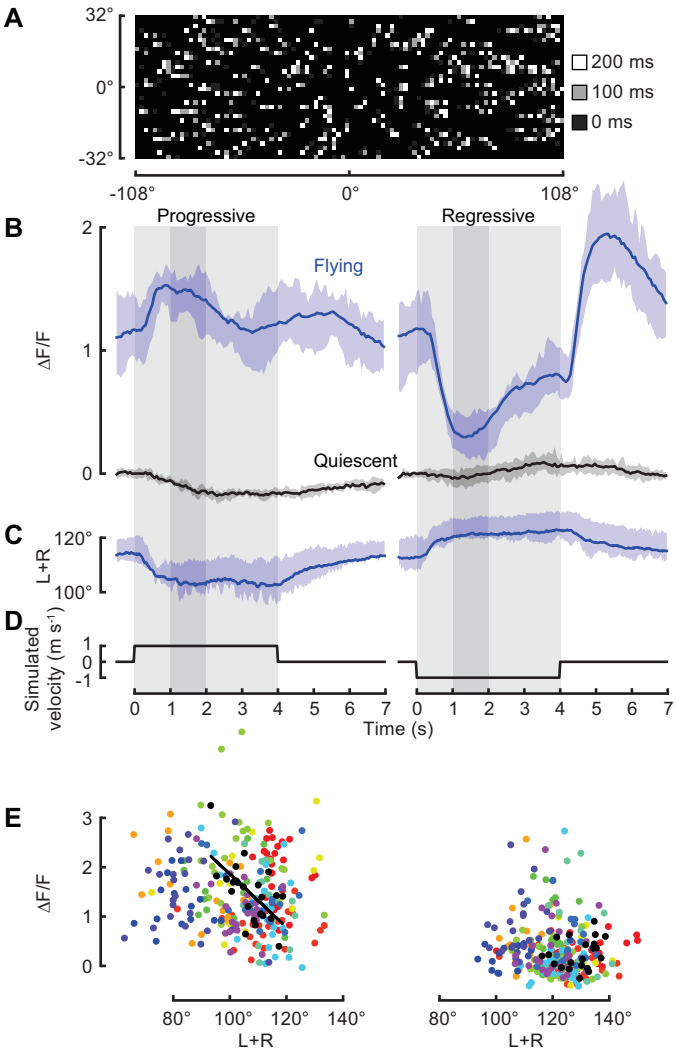
A
32°
0°
-32°
-108°
0°
108°
200 ms
100 ms
0 ms
B
Progressive
Regressive
Flying
Quiescent
ΔF/F
2
1
0
C
L+R
120°
100°
D
Simulated velocity (m s⁻¹)
1
0
-1
0 1 2 3 4 5 6 7
0 1 2 3 4 5 6 7
Time (s)
E
ΔF/F
3
2
1
0
80° 100° 120° 140°
L+R
80° 100° 120° 140°
L+R